Statistical Analysis of CO_2 Emission Based on Road Grade, Acceleration and Vehicle Specific Power for Public Utility Vehicles: An IoT Application

Maria Gemel B. Palconit
Department of Electronics Engineering
Cebu Technological University/University of San Carlos
Cebu City, Philippines
mariagemelpalconit@gmail.com

Warren A. Nuñez
Department of Electrical and Electronics Engineering
University of San Carlos-Talamban Campus
Cebu City, Philippines
warrennunez@gmail.com

***Abstract*— In the Philippine transport, the public utility vehicles (PUVs) are one of the top emitters of CO_2 emissions (CO_2e). Moreover, the need of quantifying the CO_2e of PUV is important in reducing the emission. Hence, this paper focuses on the statistical evaluation of CO_2e of PUV based on the parameters affecting it —road grade, acceleration, and vehicle specific power (VSP). An Internet of Things (IoT) system with onboard CO_2 sensors, GPS receivers, wireless communication nodes and a base station, online elevation query, cloud server, and an online IoT monitoring dashboard were used to remotely gather, store and visualize the needed measurements. The correlations of CO_2e according to these parameters were analyzed using statistical tools—histograms, box plots, and scatter plots. Results have shown that the correlation of PUV CO_2e with respect to downhill roads, uphill roads, and acceleration follows a U-shaped curves with the trough from the ranges of -19% to -3% at -16%, 3% to 22% at around 13% to 16%, and from -4m/s2 to 3m/s2 at -2m/s2, respectively. Likewise, significant changes of CO_2e were observed at different levels of VSP. Evidently, the mentioned factors have significantly affected the CO_2e of the PUVs.**

Keywords—CO_2 Emission, Internet of Things, Mobile Sensor Communications, Statistical Tools

I. Introduction

The increase of CO_2 (carbon dioxide) emission has posed an irreversible threat to the environment—global warming, the rise of sea level and climate change [1]. Aside from the negative environmental impacts, it has been also linked to causing harmful effects to human health [2]. Significantly, the greenhouse gasses (GHG) which emitted from transportation sector is one of the major contributors to the climate change [3], [4]. In addition, more than 75% of these gases contain CO_2 [3]. With this, several initiatives and schemes were made to reduce CO_2 emission in various sectors including the transportation [5].

In Philippine transportation, the public utility vehicles (PUVs) particularly the jeepneys are accounted for 80% of vehicle kilometer traveled (VKT). Hence, jeepneys are projected to obtain the highest contribution of CO_2 emission in road transport by 2035 without intervention [6]. However, ten out of twelve jeepney manufacturing companies are using 4BC2 surplus or second-hand Japanese engine. Philippine Isuzu has reported that only brand new 4JB1 and 4HF1 have complied with the Euro 1 and Euro 2 emission standards. Unfortunately, 4BC2 engines cannot only pass with Euro standards but also with the emission standard set by the Philippine Clean Air Act. It has been that only 31% of tested public utility vehicles have passed based on the Department of Environment and Natural Resources (DENR) emission standard [7]. Thus, by resolving issues of CO_2 emission in PUVs or jeepneys alone, there will be a significant reduction of the overall CO_2 in the transport sector.

Additionally, the road grade beyond eight percent obtains higher CO_2 emission [8], [9] and vehicle's sudden stop and start [10], [11] can increase the CO_2 emissions. Thus, this study focuses on the statistical evaluation of data from CO_2 measuring instrument and its correlation to road grade and acceleration. This paper also describes on how the CO_2 emission correlates to the calculated vehicle specific power (VSP) in which its input includes the road grade and vehicle's variable driving patterns such acceleration and speed [8], [12].

The most reliable onboard emission testing equipment used is the portable emissions measurement systems (PEMS) which measure several pollutants emitted from the tailpipes of the vehicle. It uses GPS to track the vehicles' location and an onboard diagnostic (OBD) port of the modern vehicles to access the data vehicle's built-in measured data such as the speed, acceleration, and temperature [13]. However, in this study, the monitoring system is implemented to PUVs wherein there is no OBD port to access the vehicles' dynamics such as speed and acceleration. Nowadays, with the availability of low-cost sensors and microcontrollers, it is possible to collect the vehicle driving profiles.

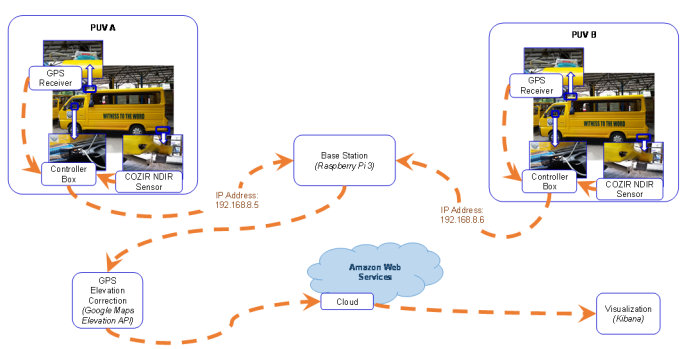

Fig. 1: System Overview

Engineering Research and Development for Technology | Department of Science and Technology

978-1-4673-9944-9/18/$31.00 ©2018 IEEE

Although, external sensors such as speedometer or accelerometer can be used to measure these parameters, this study aims to use less sensors to lessen the complexity of the monitoring system such integration of these sensors to microcontroller, the error created during few milliseconds gap in reading from the sensors, and the validation and calibration methods for each sensors. Hence, this study has decided to use the GPS not only to track the location of the vehicle but also used to measure the speed and acceleration of the vehicle.

The system was conducted to the two gasoline-fueled PUVs at the University of San Carlos wherein the campus' road grade ranges from -22% to 22%. The GPS receivers were used to track the location and vehicle dynamics while a NDIR (non-dispersive infrared) sensors were utilized to gather the CO2 emissions from the tailpipes of PUVs. Before the deployment, these sensors were validated and calibrated to ensure the reliability of the sensor readings. Among these parameters, the GPS readouts of altitudes were erratic. This has caused erroneous calculation of slope when used as a reference. With this, the altitude readouts from GPS were corrected using a free online elevation query named Google Maps Elevation API.

To make the system dynamic and smart, an Internet of Things (IoT) [14] was utilized for monitoring purpose which uses IEEE 802.11 standards for the wireless peer-to-peer (P2P) transmission and receiving scheme between the PUVs and the base station. This study also used the cloud as an online server wherein the received data from the base station were synced to the cloud server named Amazon Web Services (AWS). In this way, the collected data from two PUVs can be remotely accessed online—anytime and anywhere using the Internet. Finally, to complete the monitoring system, the data from the cloud server were visualized using a free IoT analytics named Kibana. It displays the statistical graphs of the data from the cloud server. It can also accommodate customized data searches and enables numerical download and graphical displays.

Generally, this paper describes the statistical evaluation of the gathered data using IoT system for the measurement of CO_2 emission based on road grade, VSP, and acceleration using two PUVs at the University of San Carlos. The data collection, processing, integration, and online visualization are done through the aid of Internet of Things.

Fig. 2: Vehicle Route in Pink Outline, Base Station and PUV Terminal at the University of San Carlos

II. METHODOLOGY

A. The System

The GPS receivers (Neo u-blox 6) and CO_2 NDIR (COZIR-WR) sensors were deployed to two gasoline-fueled PUVs at the University of San Carlos to gather the needed measurement every second. These sensors were wired to the controller using ESP-12E module—a microcontroller with built-in Wi-Fi transceiver which was responsible for the communication between the data gathered from the PUVs to the base station. The controller gathered the data when the PUV was routing around the campus and switched as a web server when the PUV goes back to the terminal. The base station was placed at the terminal of the PUV using Raspberry Pi 3. It was responsible for fetching the data from the PUV's broadcasted web server by accessing its URL address—http://192.168.8.5 and http://192.168.8.6 for PUV A and PUV B, respectively. Fig. 1 shows the system overview while Fig. 2 shows the route and terminal of PUV inside the campus and the base station.

The raw data from the PUV includes the PUV ID, CO_2 emission from vehicle's tailpipe, and the readout from GPS—date, time, latitude, longitude, altitude, speed and the number of satellites. Once the raw datasets were fetched by the Raspberry Pi 3, the altitude readout from GPS was corrected using the Google Maps Elevation API based on the latitudes and the longitudes. After that, these data sets with corrected elevations were processed to calculate the road grade and acceleration and were saved the Raspberry Pi's hard drive in .csv format. Also, the Raspberry Pi checked every five seconds if there was newly created processed data so that it can be synched to the Amazon Web Services—a cloud server. Finally, the synced data from the cloud were also synced to the Kibana dashboard for data visualization wherein it can be remotely accessed using the Internet.

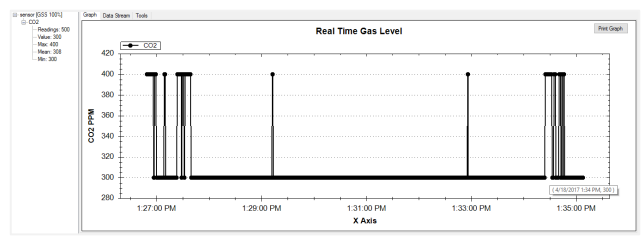

(a)

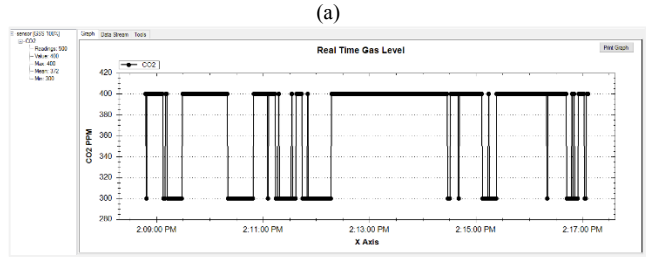

(b)

Fig. 3: Logged Data after the Configuration of COZIR NDIR Sensors using Gaslab v2.0.8.14 software: a) Sensor A; b) Sensor B

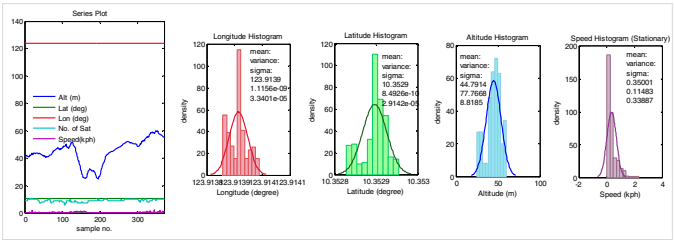

(a)

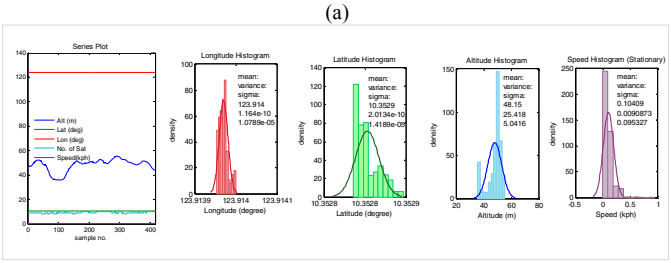

(b)

Fig. 3: Validation Result of GPS in one of the Validated Locations Using Series Plot, Histogram and Standard Deviation: a) GPS A; b) GPS B

B. *The Validation of Sensors*

In this study, the calibration of CO_2 NDIR sensor used the zeroing method in ambient air wherein the sensors were placed outside the Bunzel Building at the University of San Carlos and recorded the 500 sampled readings after it is configured to 400 ppm. The logged readings were evaluated by taking its mean value. At ambient air, reading variation around 400 ppm to 500 ppm is acceptable.

The repeatability of GPS receivers' readings was statistically validated using standard deviation and histogram. To gather the needed data, the GPS receivers were placed stationary in certain locations inside the campus. It was set to read the raw data at one hertz for about five minutes. These readings are the latitude, longitude, elevation, and speed at rest wherein the data were according to National Marine Electronics Association (NMEA) format and were analyzed using the Matlab software. The speed in motion was also validated by placing the GPS at the top of a vehicle with a maximum speed of 50 km/h. The speed was validated by correlating its distance covered in every second using linear regression with reference equation of $y = 3.6x$. Note that the speed is required for the calculation of the acceleration, hence its accuracy needs to be defined.

C. *Data Analysis*

The gathered data were analyzed using the standard deviation, RMSD (root mean square deviation), histogram, box plot, heat map, scatter plot and line graph.

TABLE I. EXAMPLE OF CORRECTED ELEVATION OF GPS READING USING GOOGLE MAPS ELEVATION API

Latitude Reading from GPS *(degrees)*	Longitude Reading from GPS *(degrees)*	Elevation Reading from GPS *(meters)*	→	Elevation from Google Map Elevation API *(meters)*
10.353121	123.914047	54.000000	→	38.205898
10.353166	123.914009	52.200001	→	38.140747
10.353185	123.914001	51.599999	→	38.106976
10.353345	123.914040	51.799999	→	38.318085
10.353587	123.914062	50.200001	→	39.041859

III. RESULTS AND DISCUSSIONS

A. *Result of Validated Sensors and Reading Correction*

The reading of COZIR NDIR sensor A was logged and plotted as shown in Fig. 3.a, it obtained 308 ppm mean value with a total of 500 logged readings at ambient air. Fig. 3.b shows that the result of the reading of sensor B for CO_2 concentration in ambient air. As can be seen, with a total of 500 logged readings, it obtains 372 ppm mean value. Note that readings around 300 ppm to 400 ppm for ambient or outdoor air is acceptable in the application in this study since its resolution is 100 ppm with a maximum measuring capacity of 1,000,000 ppm.

Whereas the validation of GPS resulted to obtain acceptable repeatability in all the measured parameters except for the altitude or elevation readings. This is shown in Fig. 3 wherein both GPS A and GPS B obtained standard deviation for longitude and latitude are within the range around 10^{-5} degrees, and the speed less than one km/h. It is also noticeable in the series plots that these parameters are plotted in a smooth horizontal line. However, the altitude readings are highly erratic as noticed in the series plots for both GPS A and B. Upon looking at the histogram, the evaluated standard deviation is around five to eight meters. This would result in a calculation of road grade from -1,948% to 1,079% when in fact, based on Google earth profile, the road grade inside the university is only about -22% to 22%. To cope with this problem, the correction for the elevation in a location was implemented using Google Maps Elevation API. Table shows the correction of elevation reading of GPS using the Google Maps Elevation API. With this, the result road grade calculation is comparable to Google Earth.

The result of the validation of the GPS reading at varying speed with one-second update interval is shown in Fig. 4. It obtains the regression equation of y = 3.6167x—0.4012 from 1156 sample point wherein its coefficient of determination is 0.9666. This means that the actual GPS reading is close to the fitted regression equation. Moreover, the RMSD between the actual data and the theoretical equation y = 3.6x is 0.0063. The result indicates that the validation of the reading of GPS for varying speed at one-second update interval is acceptable. Thus, no correction or additional sensor was initiated in this for gathering the data for speed in motion.

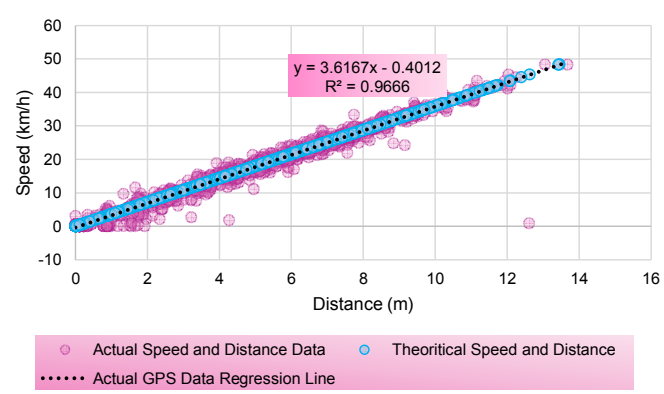

Fig. 4: Combined Validation Result for GPS A and B Reading with Variable Speed at One Second Update Interval

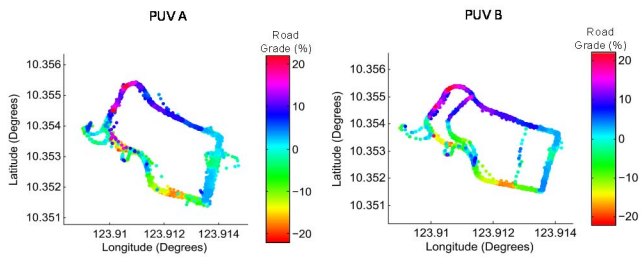

Fig. 5: Gathered Road Grade Profile from PUV A and B at the University of San Carlos

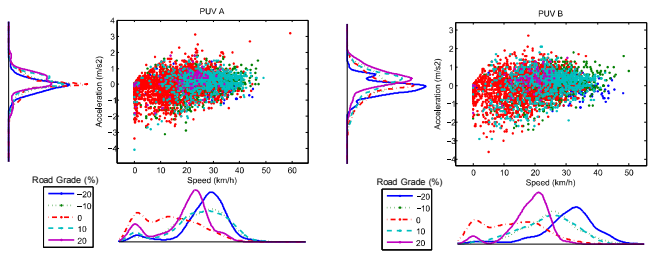

Fig. 6: Scatter Plot between Acceleration and Speed with Corresponding Distribution of Road Grade for PUV A and PUV B

B. *Profiles of the Measured Parameters—Road Grade, Speed, Acceleration and VSP*

Using the GPS receiver and the Google Maps Elevation API, the road grade profile inside the campus was obtained. As can be seen in Fig. 5, about -22% to 22% of road grade ranges were gathered for both PUV A and PUV B. Moreover, the heat map also shows that both PUV A and PUV B obtained the same road grade profile in every location.

The relationship between speed and the computed acceleration are also shown in Fig. 6 using the scatter plot. Moreover, in the same figure, the distribution of slope according to speed and acceleration are also shown using the fitted histogram curves. At different levels of road grades, the acceleration is at its peak at 0 m/s^2. Around zero percent road grade, the speeds are mostly at around 0 to 30 km/h whereas, as the road grade level tends to decrease, its peak speed increases. Such characteristics are also both observable in PUV A and PUV B.

Fig. 7 shows the correlation of VSP, acceleration and road grade. Equation (1) is used to calculate the VSP [8], as in:

$$VSP = va\delta_i + g\sin(\theta)v + C_0\, v + (1/2)\, \rho_a\, F_a\, A/M\, v^3 \qquad (1)$$

where,

v, vehicle speed (m/s); a, acceleration (m/s^2); δ_i, inertia factor; g, acceleration gravity (m/s^2); θ, road grade (rad); C_O, rolling resistance, (m/s^2); ρ_a, air specific gravity (kg/m^3); F_a, vehicle aerodynamic (N); A, vehicle frontal section (m^2); M, vehicle inertia (kg)

As observed in the figure, the increase of acceleration and road grade will cause the VSP to also increase. Moreover, most of these plots have densely occurred at around steady pace (0 m/s^2).

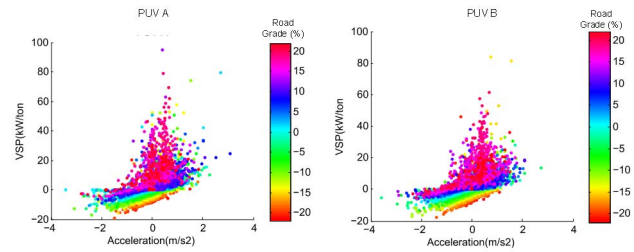

Fig. 7: PUV A and PUV B Scatter Plots for the VSP, Acceleration and Road Grade

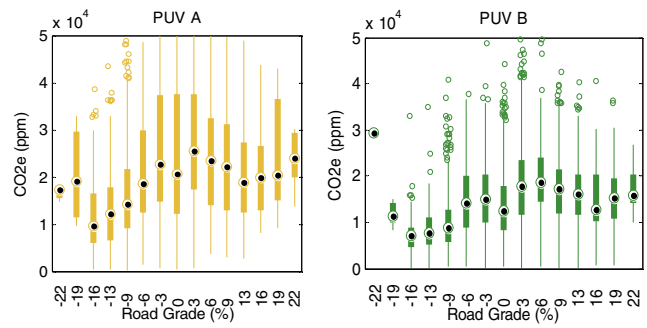

Fig. 8: Correlation of CO_2 Emission and Road Grades using Box Plot for PUV A and PUV B

Generally, the measured profiles from both PUV A and PUV B have obtained the same trends using the GPS receiver only with the corrected data for elevation using an online elevation query API. With this, it can be said that the vehicle's dynamics (acceleration, speed and VSP) inside the campus are almost identical with respect to constant entity such as the road grade, the road humps and the road's curves; this has also caused the speed to be limited to only 50 km/h.

C. *The Correlation of PUVs' Tailpipe CO_2 Emissions with Respect to Road Grades, Acceleration and VSP*

a) PUV CO_2 Emissions and the Road Grades

The CO_2 emissions according to the road grades are shown in Fig. 8 using box plot. Upon looking at the medians of the box plots, both PUV A and PUV B have almost similar trends from -19% to 22% road grades. Note that the box plot in -22% from PUV A and PUV B are different because the gathered samples in this level were few. The negative road grades from -19% to -3% has formed a U-curve trend with respect to the CO_2 emission wherein the lowest emission hits at around -16%. This curve is true for both PUV A and PUV B. Likewise, in the positive road grades from 3% to 22%, U-curve trend was also observed with lowest median plots at around 13% to 16% with respect to the CO_2 emissions. However, the CO_2 emissions at the positive road grades are consistently higher compared to the CO_2 emissions at the negative road grades for both PUV A and PUV B. Hence it can generally be said that the CO_2 emission of positive road grade is higher compared to the CO_2 emission of negative road grade. At zero percent road grade or at flat roads, the CO_2 emission lies between the average of the negative and the positive road grades.

Overall, the negative road grades, flat roads, and negative road grades have low, medium and high PUV tailpipe CO_2 emission, respectively.

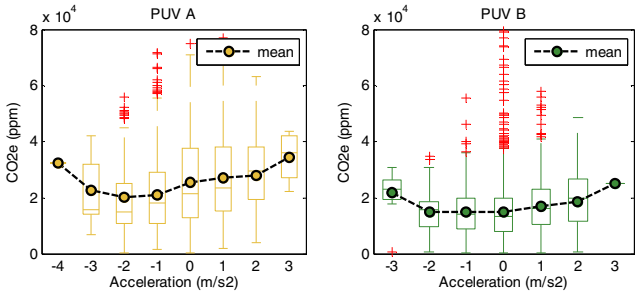

Fig. 9: Correlation of CO_2 Emission based on the Acceleration using Box Plots and Mean Values for PUV A and PUV B

b) PUV CO_2 Emission and the Acceleration

The CO_2 emissions from the tailpipes of PUV A and PUV B with respect to the acceleration are described in Fig. 9. Based on the figure, the U-curve trends were also observed for the mean values of CO_2 emission according to the acceleration. That is, the more the vehicle accelerates or decelerates, the higher CO_2 are emitted from the PUV's tailpipe. Specifically, the troughs of CO_2 emissions in PUV A and PUV B are at around -2 m/s^2 but not at 0 m/s^2. Note that the acceleration beyond -2 m/s^2, the CO_2 emission has increased for both PUV trends. Based on the graphs, the ideal driving to obtain lower CO_2 emission should be around slow slowing to steady speed driving and not abrupt speeding or slowing.

c) PUV CO_2 Emission and the VSP

The VSP of a vehicle is also widely used to correlate the CO_2 emission. Fig. 10 shows the box plots of VSP according to the PUVs' CO_2 emission. The trend shows an inverted U-curve for PUV A and PUV B. The maximum CO_2 emissions for PUV A and PUV B are 0 kW/ton and 10 kW/ton, respectively.

Generally, the VSP is classified into 14 modes [8]. However, in this paper, we will only classify it into three general classes as shown in Table II. Using the three classifications, the calculated VPS resulted to almost equal occurrence for class A (decelerating/negative road grade) and class C (accelerating/cruising/positive road grade) for both PUV A and PUV B as shown in Fig. 11.

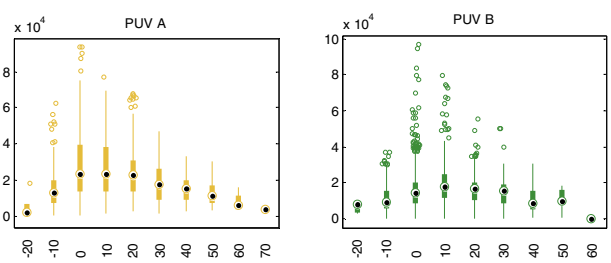

Fig. 10: Correlation of PUV CO_2 Emission and the Vehicle Specific Power (VSP) using Box Plot

TABLE II. CLASSIFICATION OF VSP

Class	Description	VSP Specifics (kW/ton)
A	Decelerating / Negative Road Grade	$-\infty \leq VSP < 0$
B	Idling	$0 \leq VSP < 1$
C	Accelerating / Cruising/ Positive Road Grade	$1 \leq VSP < \infty$

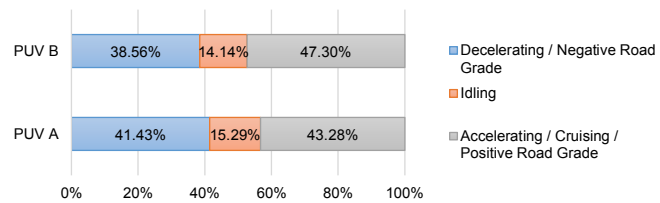

Fig. 11: Sharing of Frequency Occurrence of VSP using the Three Classifications

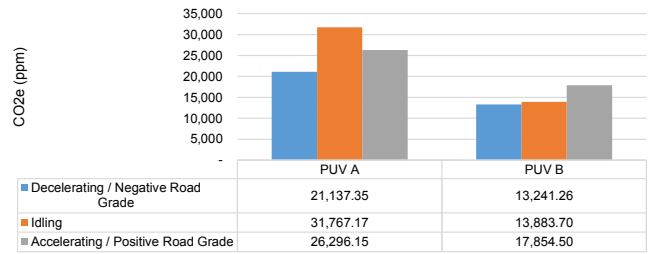

Fig. 12: Mean Values of CO_2 Emissions Based on Three Classifications of VSP for PUV A and PUV B

Note that in this study, minimal idling or stopping was observed because during the deployment, no passengers were allowed to ride the vehicle to avoid variation of CO_2 emission due to the added weight of the passenger to the vehicle. Hence, the occurrence frequency of idling is only about 14% to 15% share.

The mean values of the PUV CO_2 emissions based on three classes of VSP are shown in Fig. 12. As observed, class C has higher PUV CO_2 emission compared to the class A. Specifically, the class C is higher than class A by 20% and 26% for PUV A and PUV B, respectively. However, the CO_2 emission in class B (idling) in PUV A and PUV B are inconsistent such that in the former, the idling has the highest mean value of CO_2 emission compared to other classes whereas, in the latter, the mean of CO_2 emission is in between class A and Class B.

IV. CONCLUSION

The data gathering of this system were materialized with the help of the following: IoT—using sensors, communication nodes, and a base station; Google Maps Elevation API to correct the elevation readouts from GPS; AWS as a cloud server to sync the data from the base station for an online data access; and, Kibana to visualize the gathered data online. Moreover, the CO_2 NDIR and GPS receiver were the only sensors used in this study and no other external sensors were added to measure driving dynamics such as speed and acceleration.

The measured parameters such as road grades, acceleration and VSP have similar trends for both PUV A and PUV B. With regards to correlation of these parameters to the PUVs tailpipe CO_2 emissions, the negative, zero and positive road grades obtained low, medium and high PUV CO_2 emission, respectively. Moreover, the CO_2 emission of the positive road grades and negative road grades resulted to a U-curve pattern, i.e, its trough from -19% to -3% is at -16%, and from 3% to 22% is at around 13% and 16%, respectively.

Likewise, the trends of PUV A and PUV B's CO_2 emissions are also in a U-shaped curve wherein the trough of both PUV's acceleration from -4 m/s^2 to 3 m/s^2 is at -2m/s^2. Hence, in this study, the ideal acceleration in which the PUV emits lowest CO_2 is at -2m/s^2 and that either abrupt slowing or speeding can cause an increase of PUV CO_2 emission.

The VSP at class A which is described as the decelerating/downhill road emits lower CO_2 by 20% to 26% compared to the class C which is described as accelerating, cruising/uphill road. However, the CO_2 emission according to idling is not consistent whether it is higher or lower compared to other VSP classes. This may be due to few occurrence frequency of vehicle's stoppage during deployment. Hence, this study recommends further study of quantifying the CO_2 emission based on idling by increasing the vehicle's idling time.

APPENDIX

THE EXISTING VEHICLE EMISSION MONITORING SYSTEMS

To date, measurements of vehicle emissions such as carbon dioxide, carbon monoxide, particulate matter, hydrocarbons and nitrogen oxides can be made either in controlled conditions or in real-world conditions. In controlled conditions, vehicles are to be tested in laboratories using the chassis and engine dynamometer, which are regarded with highest accuracy results among other measuring technologies. In real-world conditions, vehicle emission measurements can be done using any of these four—remote sensing, tunnel, on-road and onboard measurements. Remote sensing measures the concentration ratios for each exhaust plume of passing vehicles. On-road measurement is done by having a mobile laboratory such as a van following an individual vehicle to capture the emissions. The tunnel measures pollutants by detecting the total flux emitted from vehicles passing in a tunnel. While portable emissions measurement systems (PEMS) are used to collect an onboard emission data and location of a vehicle [15].

It is interesting to take a deeper look at PEMS' structures because of its ability to gather an onboard measurement of gas emissions. PEMS unit is composed of gas analyzers placed in the tailpipe of a vehicle, global positioning system (GPS) to locate the vehicle and a link to onboard diagnostic (OBD) port of a vehicle to access data such vehicle and engine speed, temperature, throttle, and an onboard computer to integrate all the gathered data [15]. The gas analyzers of PEMS are using the following sensors: (i) HFID (heated flame ionization detection) to measure hydrocarbon, (ii) NDUV (non-dispersive ultraviolet) to measure nitric oxide and nitrogen dioxide, and (iii) NDIR (non-dispersive infrared) to measure CO and CO_2 [13].

ACKNOWLEDGMENT

The authors would like to acknowledge their colleagues in the University of San Carlos who contributed in finishing this study, Engineering Research and Development for Technology (ERDT) for the funding, and the PUV drivers at the University of San Carlos for allowing the authors to deploy their system to their PUVs. Above all, to God for everything.

REFERENCES

[1] S. Solomona, G.-K. Plattnerb, R. Knuttic and P. Friedlingsteind, "Irreversible climate change due to carbon dioxide emissions," *Proceedings of the National Academy of Sciences of the United States of America*, vol. 106, no. 6, p. 1704–1709, 2008.

[2] S. Chaabouni and K. Saidi, "The dynamic links between carbon dioxide (CO2) emissions, health spending and GDP growth: A case study for 51 countries," *Environmental Research*, vol. 158, pp. 137-144, 2017.

[3] S. Nocera and FedericoCavallaro, "Policy Effectiveness for containing CO2 Emissions in Transportation," *Procedia - Social and Behavioral Sciences*, vol. 20, pp. 703-713, 2011.

[4] X. Cao and W. Yang, "Examining the effects of the built environment and residential self-selection on commuting trips and the related CO2 emissions: An empirical study in Guangzhou, China," *Transportation Research Part D: Transport and Environment*, Vols. 52, Part B, pp. 480-494, 2017.

[5] Z. AbdulManan, W. N. R. Nawi, S. R. Alwi and J. JaromírKlemeš, "Advances in Process Integration research for CO2 emission," *Journal of Cleaner Production*, vol. 167, pp. 1-13, 2017.

[6] H. Fabian and S. Gota, "CO2 Emissions from the Land Transport Sector in the Philippines: Estimates and Policy Implications," in *Proceedings of the 17th Annual Conference of the Transportation Science Society of the Philippines,* 2009.

[7] R. S. Bacero and K. Vergel, "Assessment of Jeepney's Components, Systems and Separate Technical Units for the Development of Standards," in *Proceedings of the 17th Annual Conference of the Transportation Science Society of the Philippines*, 2009.

[8] L. D. Ragionea, G. Meccariello, M. V. Prati and M. A. Costagliola, "Statistical evaluation of slope's effect on real emissions and fuel consumption performed with different cars in Naples urban area," in *Transport Research Arena 2014*, Paris, 2014.

[9] K. Boriboonsomsin and M. Barth, "Impacts of Road Grade on Fuel Consumption and Carbon Dioxide Emission Evidenced by Use of Advanced Navigation Systems," *Transportation Research Record Journal of the Transportation Research Board* , vol. 2319, no. 03, pp. 21-30, 2009.

[10] G. S. Larue, H. Malik, A. Rakotonirainy and S. Demmel, "Fuel consumption and gas emissions of an automatic transmission vehicle following simple eco-driving instructions on urban roads," *IET Intelligent Transport Systems*, vol. 8, no. 7, pp. 590 - 597, 2014.

[11] S. K. Pathak, V. Sood, Y. Singh and S. Channiwala, "Real world vehicle emissions: Their correlation with driving parameters," *Transportation Research Part D: Transport and Environment,* vol. 44, pp. 157-176, 2016.

[12] H. Zhai, H. C. Frey and N. M. Rouphail, "A Vehicle-Specific Power Approach to Speed- and Facility-Specific Emissions Estimates for Diesel Transit Buses," *Environmental Science and Technology,* vol. 42, no. 21, p. 7985–7991, 2008.

[13] T. Cao, T. D. Durbin, D. R. CockerIII, R. Wanker, T. Schimpl, V. Pointner, K. Oberguggenberger and K. C. Johnson, "A Comprehensive Evaluation of a Gaseous Portable Emissions Measurement System with a Mobile Reference Laboratory," *Emission Control Science and Technology*, vol. 2, no. 3, p. 173–180, 2016.

[14] J. Gubbi, R. Buyya, S. Marusic and M. Palaniswami, "Internet of Things (IoT): A vision, architectural elements, and future directions," *Future Generation Computer Systems,* vol. 29, no. 7, pp. 1645-1660, 201

[15] V. Franco, M. Kousoulidou, M. Muntean, L. Ntziachristos, S. Hausberger and P. Dilara, "Road vehicle emission factors development: *A review," Atmospheric Environment*, vol. 70, pp. 84-97, 2013.